Supplementary Information (SI) for Inorganic Chemistry Frontiers.
This journal is © the Partner Organisations 2026

Supporting Information

Bridging the Gap: Thymine Segments to Create Single-Strand Versions of DNA_2-$[Ag_{16}Cl_2]^{8+}$

Vanessa Rück,[a,1,*] Hiroki Kanazawa,[b,1] Zhiyu Huang,[a] Christian Brinch Mollerup,[c] Leila Lo Leggio,[a] Jiro Kondo,[b,*] and Tom Vosch [a,*]

a. Department of Chemistry, University of Copenhagen, Universitetsparken 5, 2100 Copenhagen, Denmark.

b. Department of Materials and Life Sciences, Sophia University, 7-1 Kioi-cho, Chiyoda-ku, 102-8554 Tokyo, Japan.

c. Department of Forensic Medicine, University of Copenhagen, Frederik V's Vej 11, 2100 Copenhagen, Denmark.

1 Contributed equally

Synthesis of 2xDNA-AgNC

Hydrated DNA oligonucleotide (Integrated DNA Technologies) was mixed with $AgNO_3$ (Sigma Aldrich, ≥ 99.998%) in 30 mM NaCl and 10 mM NH_4OAc aqueous solution (Sigma Aldrich, ≥ 98%) at pH 7. Freshly prepared $NaBH_4$ (Sigma Aldrich, ≥ 99.99%) was added to the mixture after 15 minutes to reduce the silver cations and promote the formation of nanoclusters. The optimal ratio between the components was [DNA]:[$AgNO_3$]:[$NaBH_4$] = 25 µM: 187.5 µM: 93.75 µM, according to previously published protocol.[1] After synthesis, the sample was stored in the fridge for 7 days prior to high-performance liquid chromatography (HPLC) purification. In the end, the purified fraction was solvent exchanged to 10 mM NH_4OAc by spin-filtration with a 3 kDa cut-off membrane filters (Amicon Ultracel-3) to ensure good stability of DNA-AgNCs over time.

List of used DNA sequences:

- 2xDNA(**T_4**): CAC CTA GCG A**TT TT**C ACC TAG CGA
- 2xDNA(**T_5**): CAC CTA GCG A**TT TTT** CAC CTA GCG A
- 2xDNA(**T_6**): CAC CTA GCG A**TT TTT T**CA CCT AGC GA

HPLC purification of 2xDNA(T_x)-AgNC

HPLC purification was performed using a preparative HPLC system from Agilent Technologies with an Agilent Technologies 1100 Series UV-Vis detector, an Agilent Technologies 1260 Infinity fluorescence detector, and a Kinetex C18 column (5 µm, 100 Å, 250 × 4.6 mm), equipped with a fraction collector. The mobile phase was a gradient mixture of 35 mM triethylammonium acetate (TEAA, PanReac AppliChem) buffer in MilliQ water (A) and methanol (B). The flow rate was set to 1 mL/min.

The HPLC method for 2xDNA(T_x)-AgNC was as follows: In the first 2 minutes, the concentration of B was kept constant at 25 % and then linearly increased to 50 % B in 25 minutes (ΔB = 1% B/min). Afterwards, the gradient was increased to 95% over 3 minutes and kept at the same percentage for 5 more minutes to remove any remaining sample and nanoparticles from the column.

The collection was based on the absorbance at 530 nm, while monitoring the DNA absorbance at 260 nm and the absorption of silver nanoparticles at 450 nm. The AgNC emission band was monitored at 730 nm, exciting at 530 nm. The chromatograms are shown in Figures S2-S4.

Mass spectrometry

ESI-MS measurements were performed with a Xevo G2-XS QTof (Waters Corporation, Milford, MA, USA), using negative ion mode with a 1.5 kV capillary voltage, 40 V cone voltage and no collision energy. Spectra were collected from 750 to 4000 m/z, and with a scan time of 1 second. Source temperature was 100 °C with a cone gas flow of 50 L/h, and the desolvation temperature and gas flow were 350 °C and 800 L/h, respectively. The QTOF was calibrated using ESI-L Low Tune Mix (Agilent Technologies, Santa Clara, CA, USA), which contained compounds for negative mode in the mass range of *m/z* 113 to 2834. All samples were injected using an Acquity I-Class Plus system (Waters) with a flow-through needle autosampler, with a flow of 0.05 mL/min 50 mM NH_4OAc buffer at pH 7 – MeOH (80:20) and using 3 µL injection volume.

The system was operated using UNIFI v.1.9.4 (Waters), and the final spectra were generated by averaging multiple spectra surrounding the apex of the observed peak.

The recorded data were analyzed and fitted with the open-source software EnviPat Web[2] (https://www.envipat.eawag.ch/index.php).

Table S1. *Gaussian fits for the experimentally measured mass spectra (x_0^{exp}) and the corresponding theoretical mass distributions (x_0^{th}), and the absolute error calculated as $x_0^{exp} - x_0^{th}$.*

	Name	z	Chemical formula	Molecular weight	x_0^{th}	x_0^{exp}	Error
T_6	2xDNA(T_6)-$[Ag_{16}Cl_2]^{8+}$	5-	$C_{252}H_{321}N_{90}O_{156}P_{25}[Ag_{16}Cl_2]^{8+}$	9677.88	1932.94	1932.99	0.05
	2xDNA(T_6)-$[Ag_{17}Cl_2]^{9+}$	5-	$C_{252}H_{321}N_{90}O_{156}P_{25}[Ag_{17}Cl_2]^{9+}$	9785.75	1954.31	1954.35	0.04
T_5	2xDNA(T_5)-$[Ag_{16}Cl_2]^{8+}$	5-	$C_{242}H_{308}N_{88}O_{149}P_{24}[Ag_{16}Cl_2]^{8+}$	9373.69	1872.10	1872.13	0.03
	2xDNA(T_5)-$[Ag_{17}Cl_2]^{9+}$	5-	$C_{242}H_{308}N_{88}O_{149}P_{24}[Ag_{17}Cl_2]^{9+}$	9481.56	1893.47	1893.51	0.04
T_4	2xDNA(T_4)-$[Ag_{16}Cl_2]^{8+}$	5-	$C_{232}H_{295}N_{86}O_{142}P_{23}[Ag_{16}Cl_2]^{8+}$	9069.50	1811.26	1811.31	0.05
	2xDNA(T_4)-$[Ag_{17}Cl_2]^{9+}$	5-	$C_{232}H_{295}N_{86}O_{142}P_{23}[Ag_{17}Cl_2]^{9+}$	9177.37	1832.64	1832.66	0.02

Absorption measurements:

Absorption spectra were carried out on a Cary 3500 Flexible UV-Vis spectrophotometer from Agilent Technologies using a Xenon flash lamp for visible and near-infrared radiation. The measurements were performed in a single-beam configuration with a baseline correction. Every spectrum was subtracted by the corresponding blank absorption spectrum.

Steady-state emission measurements:

Steady-state fluorescence measurements were performed using a FluoTime300 instrument (PicoQuant). The fluorescence spectra were recorded by exciting the samples with a vertically-polarized 507.5 nm (LDH-PC-510, PicoQuant) picosecond-pulsed laser. All emission spectra have been corrected for the wavelength dependency of the detector.

Quantum Yield (Q) measurements and calculations:

The quantum yield was measured in two ways. First, the relative method was used to determine the quantum yield of 2xDNA(T_6)-AgNC in 10 mM NH_4OAc aqueous solution at 25 °C, using DNA-Ag_{16}NC in 10 mM NH_4OAc aqueous solution as reference dye (Q_{ref} = 0.26).[1] Absorption and emission spectra of the DNA-AgNC and the reference compound were measured at five different concentrations, and the quantum yield was calculated according to the following formula:

$$Q_{NC} = \frac{F_{NC}}{f_{A,NC}} \times \frac{f_{A,ref}}{F_{ref}} \times \frac{n_{NC}^2}{n_{ref}^2} \times Q_{ref}$$

where *Q* represents the quantum yield, *F* is the integrated emission spectrum (*i.e.*, the area under the fluorescence spectrum), f_A defines the fraction of absorbed light at the excitation wavelength (507 nm), and *n* is the refractive index of the medium where the compounds are dissolved in during the measurements. The subscripts *NC* and *ref* indicate the 2xDNA(T_6)-AgNC and DNA-Ag_{16}NC, respectively. The corresponding spectra is shown in Figure S8.

For the determination of *Q* of 2xDNA(T_6)-AgNC, 2xDNA(T_5)-AgNC and 2xDNA(T_4)-AgNC a one-point method was used. DNA-Ag_{16}NC was used as a reference (Q_{ref} = 0.26).[1] Absorption and emission spectra of the DNA-AgNC were measured at one concentration, and the quantum yield was calculated as described above. The results obtained using both methods for 2xDNA(T_6)-AgNC are consistent. All values are reported in Table 1, and corresponding spectra are shown in Figure S9.

Time-correlated single-photon counting (TCSPC) measurements:

Time-resolved fluorescence measurements were performed using a FluoTime300 instrument from PicoQuant with a vertically-polarized pulsed laser at 507.5 nm (LDH-PC-510, PicoQuant) as excitation source. The integration time was chosen to be 10 s in order to reach at least 10,000 counts in the maximum at 750 nm. The data analysis was performed with FluoFit v.4.6 software (PicoQuant). The decays were fitted with a bi-exponential reconvolution model including the IRF. The amplitude (α_i) and decay time (τ_i) components were used to calculate the intensity-weighted average decay time, $\langle\tau\rangle$, reported in Table 1.

In addition, time-resolved anisotropy measurements were performed by recording both parallel and perpendicular fluorescence intensity decays at 750 nm. The samples were excited at 507.5 nm with a vertically-polarized laser (LDH-P-C-510, PicoQuant). The anisotropy data were fitted with the same software from PicoQuant, using a multi-exponential reconvolution model for the decay time and a mono-exponential function for the rotational correlation time (θ), including the IRF. The hydrodynamic volume (V_{hydro}) was then calculated according to the following equation:

$$\theta = \frac{\eta \cdot V_{hydro}}{k_B \cdot T}$$

where η is the dynamic viscosity of the solvent, T is the absolute temperature and k_B is the Boltzmann constant.

Fluorescence spectra and decay time measurements on a home-build microscope:

Emission spectra and decay time measurements were performed on our home-built confocal microscope (Olympus IX71).[3] A continuum white-light laser (SuperK EXTREME EXB-6, NKT Photonics) was used as an excitation source delivering a wavelength of 514 nm (9.735 MHz repetition rate) by sending the continuum output through an acousto-optic tunable filter (SuperK SELECT, NKT Photonics). The output of the laser was expanded and collimated by a lens system and cleaned up by several filters (LL01-514-25,FF01-520/5-25,FF01-650/SP-25 Semrock) before it was reflected by a 30:70 beam splitter (XF122, Omega Optical) and sent through an air objective (CPlanFLN 10x, NA= 0.3, Olympus). Excitation power on top of the sample was 4.5 nW. The objective that collected the fluorescence was directed through a 100 µm pinhole and a 514 nm long-pass filter (LP02-514RE-25, Semrock). The fluorescence was then sent

through a spectrograph (SP 2356 spectrometer, 300 grooves/mm, Acton Research) onto a nitrogen cooled CCD camera (SPEC-10:100B/LN-eXcelon, Princeton Instruments) for the recording of spectra. Finally, the emission spectra were wavelength and intensity corrected as reported previously.[3]

Fluorescence decay time measurements were performed on the same inverted confocal microscope. The fluorescence signal was detected by an avalanche photodiode (Perkin-Elmer CD3226) connected to a single photon counting module (Becker & Hickl SPC-830). Excitation power on top of the sample was 0.45 nW.

Crystal data collection, processing, phasing and refinement:

To determine the structure of the 2xDNA(T_5)-$[Ag_{16}Cl_2]^{8+}$ and 2xDNA(T_6)-$[Ag_{16}Cl_2]^{8+}$, we collected datasets using MicroMAX and BioMAX at MAX IV (Lund, Sweden), respectively. For both datasets, the diffraction patterns were obtained using 0.1° oscillation steps with an exposure time of 0.01 s. A total of 3600 frames were recorded. All datasets were processed with the program *XDS*.[4] The reflection data were converted by *Reflection file editor* of the *Phenix suite*.[5] The locations of silvers were partially determined by the standard direct method phasing protocol in *SIR2019*.[6] The initial phase was estimated by the program *AutoSol* in the *Phenix suite*[5] using the location of the silvers as the reference heavy atom sites. The crystal structure was constructed by using the program *Coot*.[7, 8] The atomic parameters were refined using the program *phenix.refine* in the *Phenix suite*.[5] Crystal as well as the crystallization condition for the data collection, and the statistics of structure determination are summarized in Table S2 and Table S3, respectively.

Table S2. *Crystallization conditions for X-ray diffraction data collection.*

Sample name	2xDNA(T_5)-$[Ag_{16}Cl_2]^{8+}$ and 2xDNA(T_6)-$[Ag_{16}Cl_2]^{8+}$
Temperature	293K
DNA-AgNC solution (0.5 µl):	
2xDNA(T_5)-$[Ag_{16}Cl_2]^{8+}$ or 2xDNA(T_6)-$[Ag_{16}Cl_2]^{8+}$	~ 200 µM
Crystallization solution (0.5 µl):	
Potassium nitrate	200 mM
Spermine	10 mM
3-(N-morpholino)propanesulfonic acid (pH = 7.0)	50 mM
Polyethylene glycol 3350	10%
Reservoir solution (250 µl):	
Polyethylene glycol 3350	40%
Crystals	See Figure S10

Table S3. *Crystal data, statistics of data collection and structure refinement.*

Sample name	2xDNA(T_5)-$[Ag_{16}Cl_2]^{8+}$	2xDNA(T_6)-$[Ag_{16}Cl_2]^{8}$
PDB-ID	9XV9 (pdb_00009xv9)	9XVA (pdb_00009xva)
Crystal data		
Space group	*P*4	*P*4
Unit cell (Å)	a = 77.05, b = 77.05, c = 21.51	a = 80.85, b = 80.85, c = 24.51
Z [a]	2	2

Data collection		
Beamline	MicroMAX of MAX IV	BioMAX of MAX IV
Wavelength (Å)	0.97761	1.00003
Resolution (Å)	38.52-2.0	40.42-1.7
of the outer shell (Å)	2.05-2.00	1.74-1.70
Unique reflections	16707	34153
Completeness (%)	99.4	99.7
in the outer shell (%)	98.5	98.3
R_{anom} [b] (%)	8.9	8.3
in the outer shell (%)	28.0	21.7
Redundancy	6.98	6.73
in the outer shell	6.79	6.77
Structure refinement		
Resolution range (Å)	38.52-2.0	40.42-1.7
Used reflections	16691	34135
R-factor [c] (%)	13.5	14.4
R_{free} [d] (%)	16.2	15.5
Number of DNA atoms	864	906
Number of Ag	32	32
Number of Cl	4	4
Number of water	35	46
R.m.s.d. bond length (Å)	0.010	0.010
R.m.s.d. bond angles (°)	1.6	1.6

[a] Number of DNA-AgNCin the asymmetric unit.

[b] $R_{anom} = 100 \times \Sigma_{hklj}|I_{hklj}(+)-I_{hklj}(-)| \,/\, \Sigma_{hklj}[I_{hklj}(+) + I_{hklj}(-)]$.

[c] R-factor $= 100 \times \Sigma||F_o| - |F_c|| \,/\, \Sigma|F_o|$, where $|F_o|$ and $|F_c|$ are optimally scaled observed and calculated structure factor amplitudes, respectively.

[d] Calculated using a random set containing 10% of observations.

Figures:

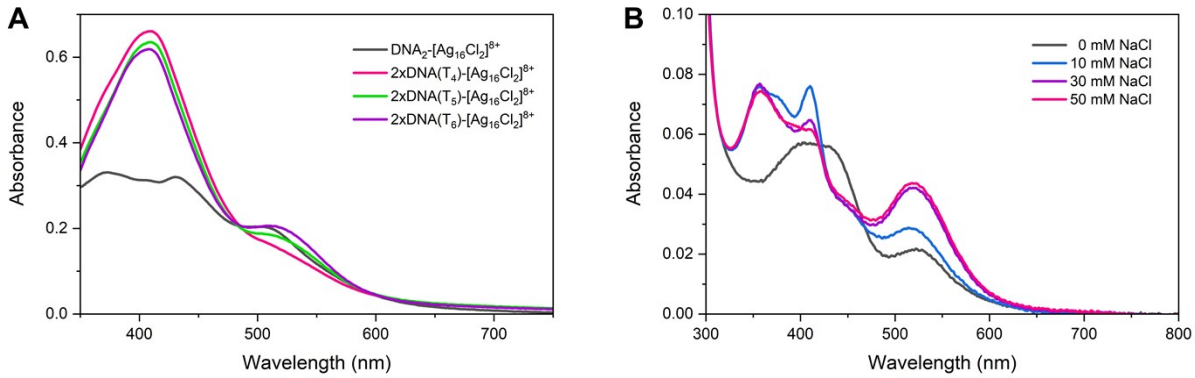

Figure S1: (A) Absorption spectra of unpurified DNA_2-$[Ag_{16}Cl_2]^{8+}$ and 2x$DNA(T_x)$-$[Ag_{16}Cl_2]^{8+}$ 5 and 7 days after synthesis, respectively, at room temperature (1 cm cuvette). (B) NaCl test. Absorption spectra of unpurified 2x$DNA(T_6)$-$[Ag_{16}Cl_2]^{8+}$ in different NaCl concentrations, 7 days after synthesis at room temperature (0.2 cm cuvette). The formation of 2x$DNA(T_6)$-$[Ag_{16}Cl_2]^{8+}$ (525 nm absorption band) can be promoted by adding NaCl.

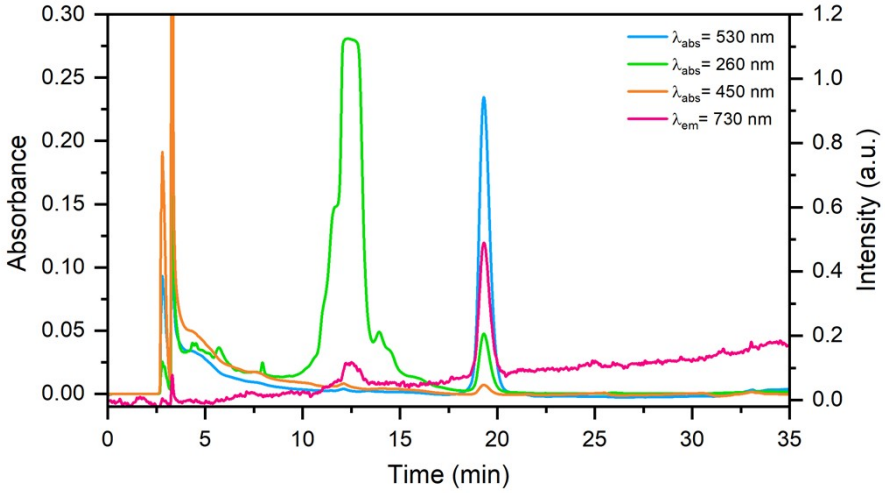

Figure S2: HPLC chromatograms of 2xDNA(T_4)-[$Ag_{16}Cl_2$]$^{8+}$ monitoring the absorption at 530 nm, 260 nm and 450 nm, and the fluorescence signal at 730 nm (exciting at 530 nm). The fraction was collected between 18.8 and 20 min (41.8-43 % B).

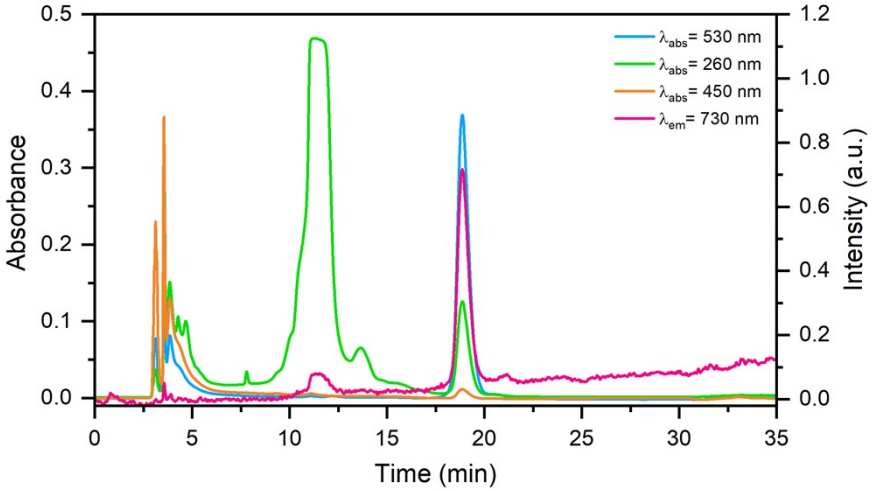

Figure S3: HPLC chromatograms of 2xDNA(T_5)-[$Ag_{16}Cl_2$]$^{8+}$ monitoring the absorption at 530 nm, 260 nm and 450 nm, and the fluorescence signal at 730 nm (exciting at 530 nm). The fraction was collected between 18.3 and 19.7 min (41.3-42.7 % B).

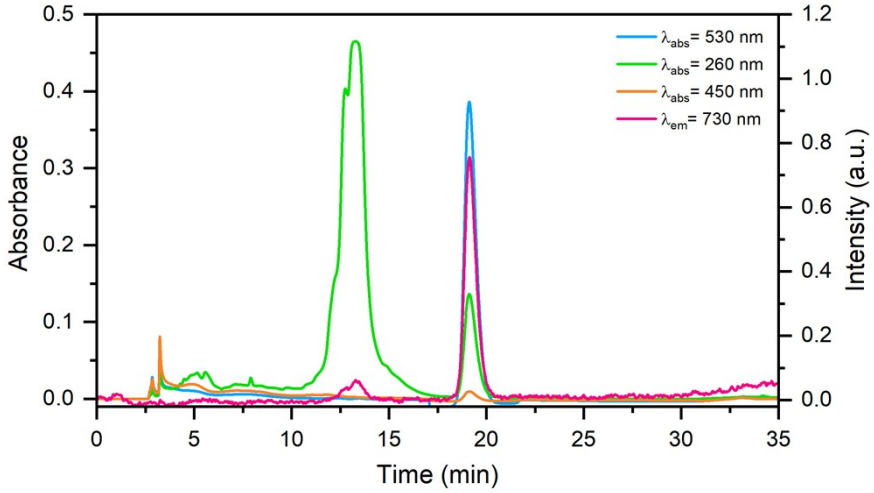

Figure S4: HPLC chromatograms of 2xDNA(T_6)-[$Ag_{16}Cl_2$]$^{8+}$ monitoring the absorption at 530 nm, 260 nm and 450 nm, and the fluorescence signal at 730 nm (exciting at 530 nm). The fraction was collected between 18.6 and 20 min (41.6-43 % B).

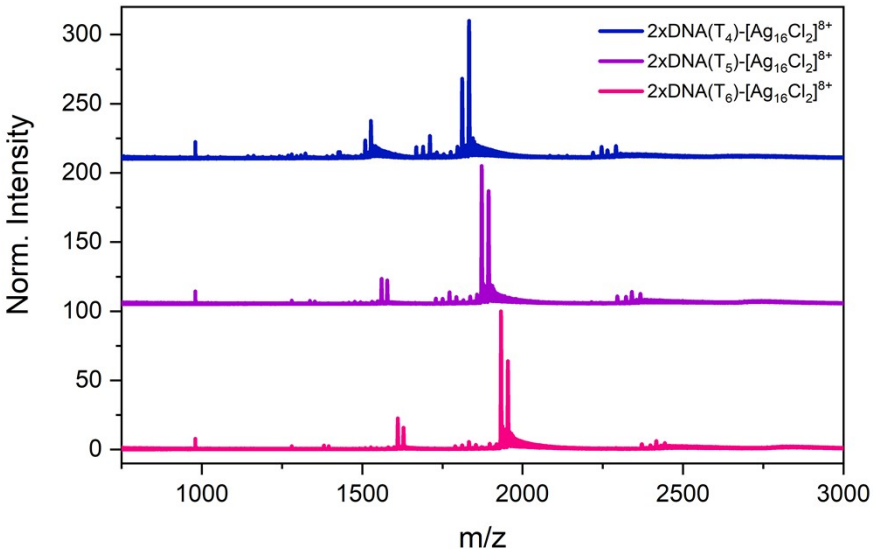

Figure S5: Mass spectra of 2xDNA(T_4)-[$Ag_{16}Cl_2$]$^{8+}$, 2xDNA(T_5)-[$Ag_{16}Cl_2$]$^{8+}$ and 2xDNA(T_6)-[$Ag_{16}Cl_2$]$^{8+}$ in 10 mM NH_4OAc at room temperature measured in negative ion mode, displayed with off-set.

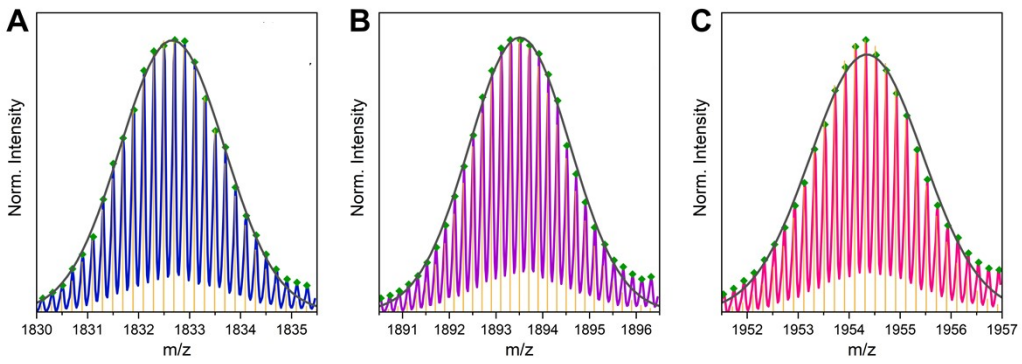

Figure S6: Theoretical isotopic distribution fits (yellow) together with experimental data for (A) 2xDNA(T_4)-[$Ag_{17}Cl_2$]$^{9+}$in blue, (B) 2xDNA(T_4)-[$Ag_{17}Cl_2$]$^{9+}$in purple and (C) 2xDNA(T_4)-[$Ag_{17}Cl_2$]$^{9+}$ in pink for z= 5- region. The dark gray line represents the Gaussian fit, while the green dots indicate the peaks used for the fit. The corresponding mean values are μ = 1832.7, 1893.5, and 1954.4 for (A), (B), and (C), respectively.

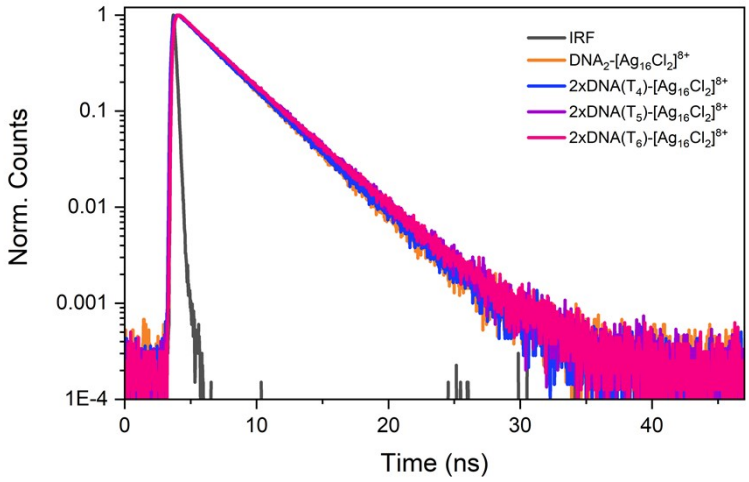

Figure S7: Fluorescence decays of DNA_2-[$Ag_{16}Cl_2$]$^{8+}$and 2xDNA(T_x)-[$Ag_{16}Cl_2$]$^{8+}$ in 10 mM NH_4OAc measured at 740 nm (λ_{exc}= 507.5 nm) at room temperature. The decays were fitted with a bi-exponential reconvolution function, and the respective intensity-weighted average decay times are reported in Table 1. The dark gray trace is the instrument response function (IRF).

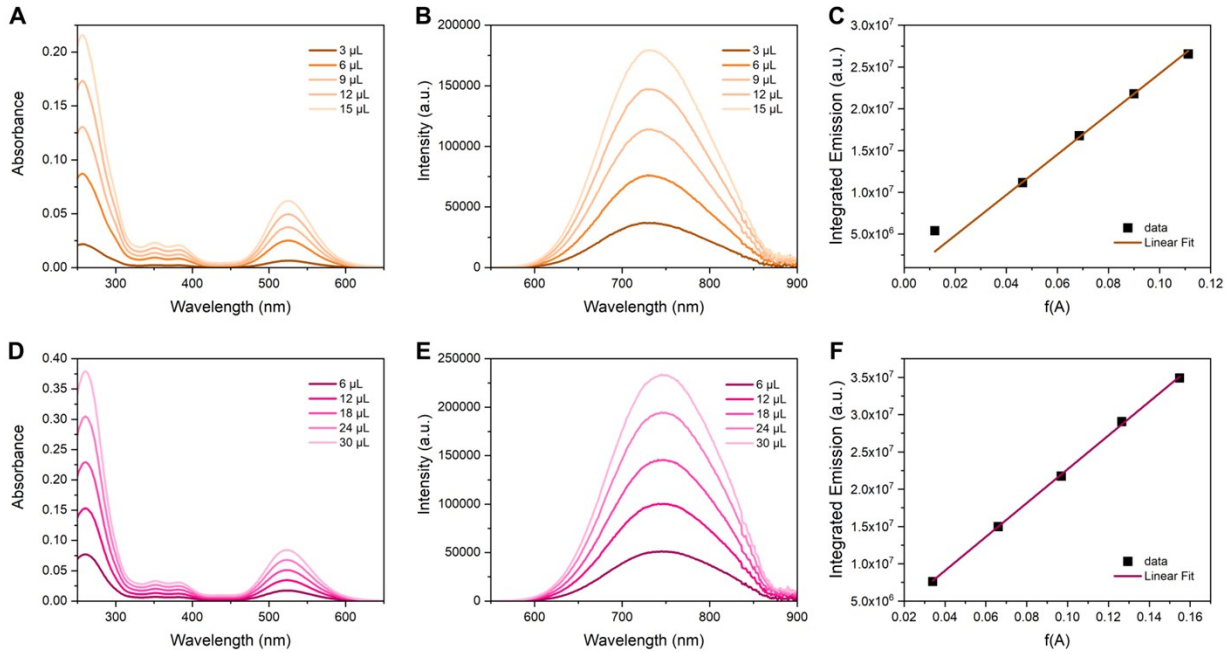

Figure S8: 2xDNA(T_6)-[$Ag_{16}Cl_2$]$^{8+}$ quantum yield determination. (A) Absorption and (B) emission spectra (λ_{exc}= 507.5 nm) of the reference DNA-Ag_{16}NCs in 10 mM NH_4OAc at 25 ˚C. (D) Absorption and (E) emission spectra (λ_{exc}= 507.5 nm) of 2xDNA(T_6)-[$Ag_{16}Cl_2$]$^{8+}$ in 10 mM NH_4OAc at 25 ˚C. (C) and (F) Zero-intercept linear fits of the integrated fluorescence vs. the fraction of absorbed light for DNA-Ag_{16}NCs and 2xDNA(T_6)-[$Ag_{16}Cl_2$]$^{8+}$, respectively. The slopes were used to calculate the Q of the sample, Q= 0.24.

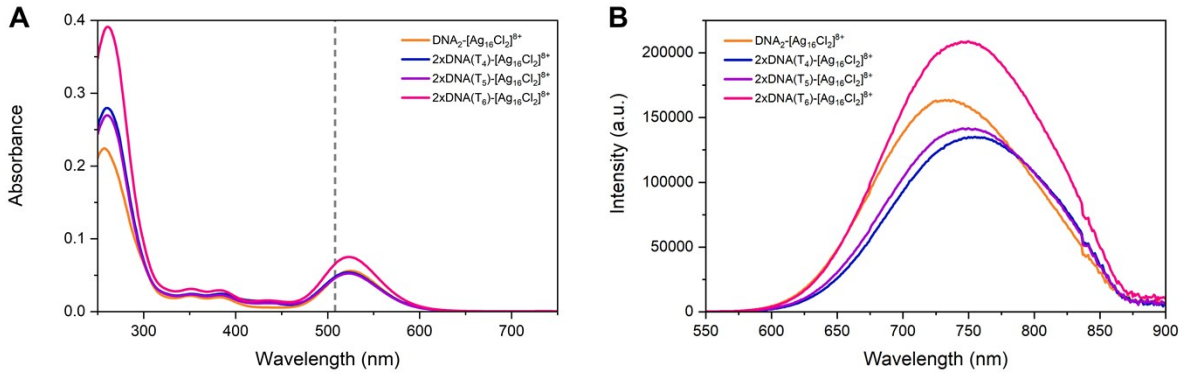

Figure S9: 1-point Quantum Yield determination for 2xDNA(T_x)-[$Ag_{16}Cl_2$]$^{8+}$. DNA_2-[$Ag_{16}Cl_2$]$^{8+}$ in 10 mM NH_4OAc was used as reference dye. (A) Absorption and (B) emission spectra (λ_{exc}= 507.5 nm) of 2xDNA(T_x)-[$Ag_{16}Cl_2$]$^{8+}$ and DNA_2-[$Ag_{16}Cl_2$]$^{8+}$ in 10 mM NH_4OAc at 25 ˚C. The calculation was carried out as described above, the values are reported in Table 1.

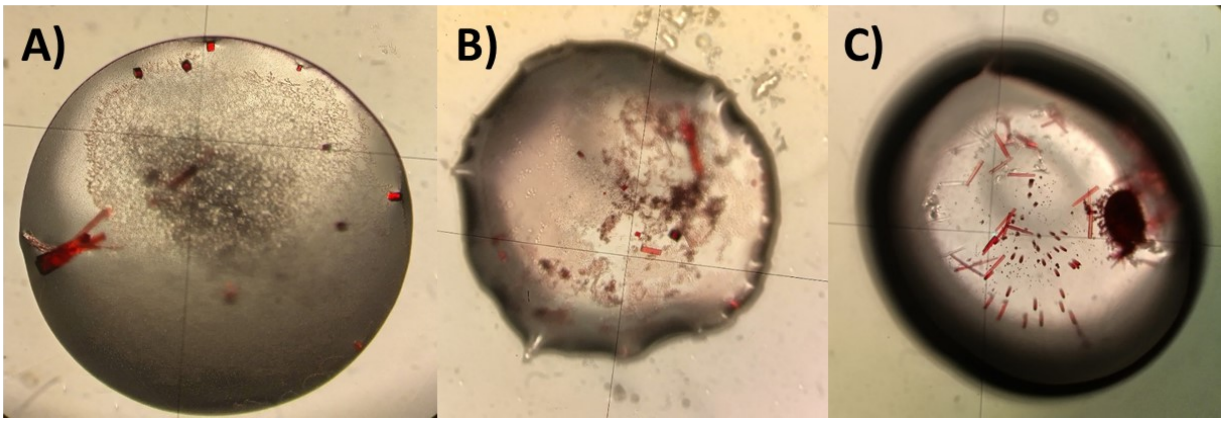

Figure S10: Images of the (A) 2xDNA(T_4)-[$Ag_{16}Cl_2$]$^{8+}$, (B) 2xDNA(T_5)-[$Ag_{16}Cl_2$]$^{8+}$, (C) 2xDNA(T_6)-[$Ag_{16}Cl_2$]$^{8+}$ crystals. All crystals were grown with 10% PEG 3350, 10 mM spermine, 50 mM MOPS and 200 mM KNO_3.

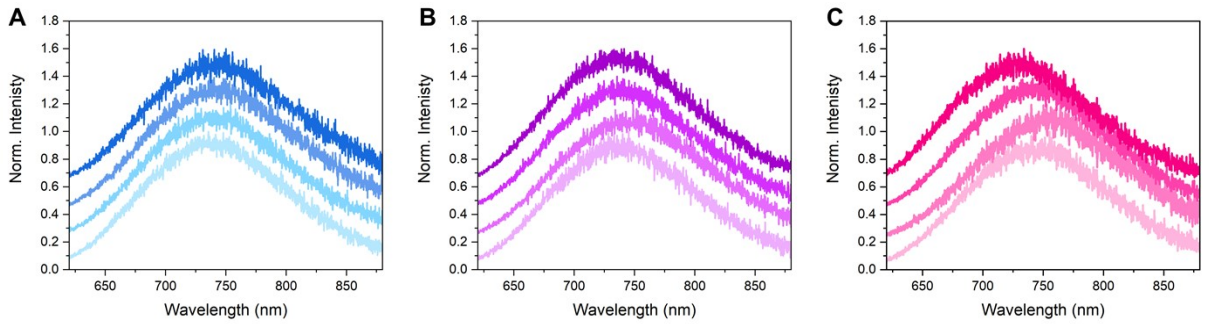

Figure S11: Emission spectra of (A) 2xDNA(T_4)-[$Ag_{16}Cl_2$]$^{8+}$, (B) 2xDNA(T_5)-[$Ag_{16}Cl_2$]$^{8+}$ and (C) 2xDNA(T_6)-[$Ag_{16}Cl_2$]$^{8+}$ crystals, exciting at 514 nm. The emission spectra are normalized to the emission maximum and have a constant 0.2 offset for displaying purposes. The crystals were grown with 10% PEG 3350, 10 mM spermine, 50 mM MOPS and 200 mM KNO_3.

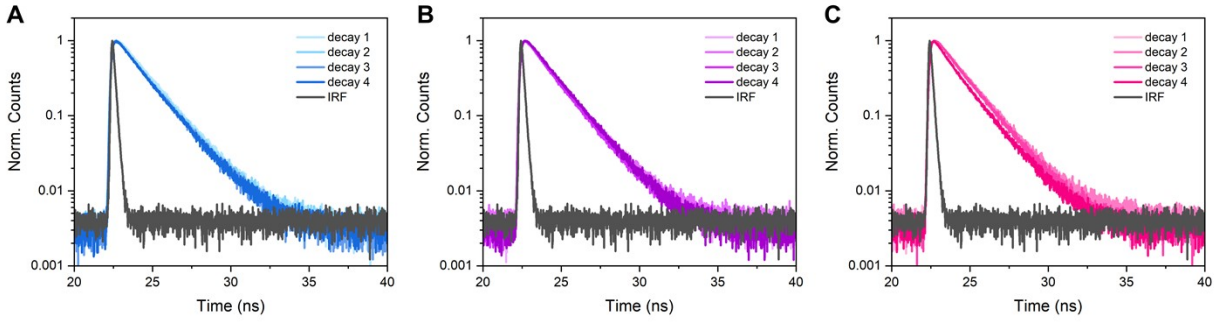

Figure S12: Fluorescence decay curves of (A) 2xDNA(T_4)-[$Ag_{16}Cl_2$]$^{8+}$, (B) 2xDNA(T_5)-[$Ag_{16}Cl_2$]$^{8+}$ and (C) 2xDNA(T_6)-[$Ag_{16}Cl_2$]$^{8+}$ crystals, exciting at 514 nm. The IRF is the dark gray line. The crystals were grown with 10% PEG 3350, 10 mM spermine, 50 mM MOPS and 200 mM KNO_3.

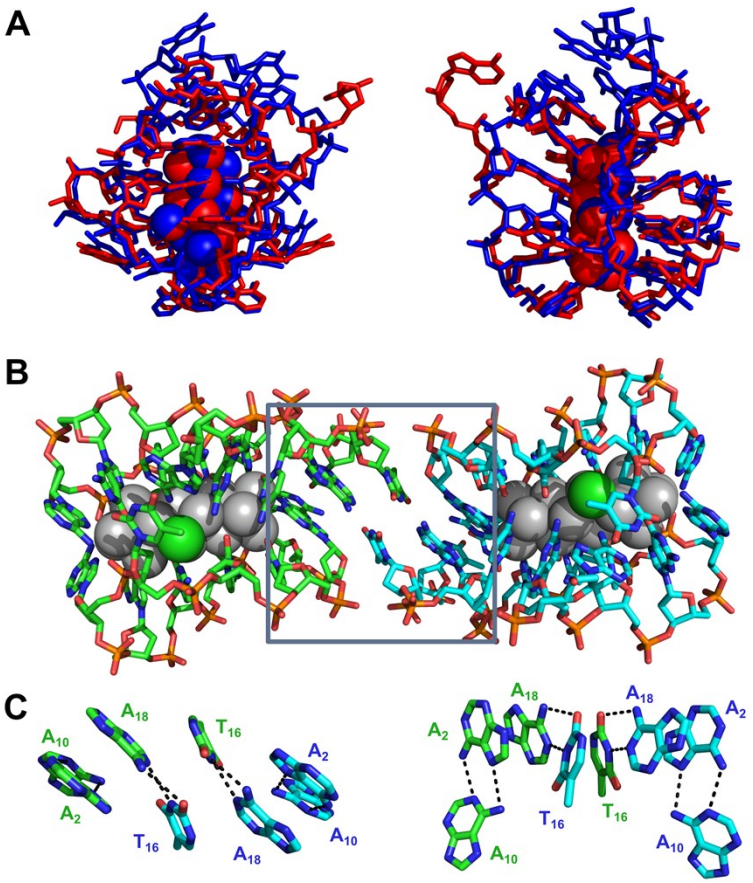

Figure S13: (A) Crystal structure overlay of 2xDNA(T_6)-[$Ag_{16}Cl_2$]$^{8+}$ (blue, PBD: 9XVA) and DNA_2-[$Ag_{16}Cl_2$]$^{8+}$ unit (red, PBD: 6JR4). (B-C) Detailed insight into 2xDNA(T_6)-[$Ag_{16}Cl_2$]$^{8+}$ structure.

References

1. S. A. Bogh, M. R. Carro-Temboury, C. Cerretani, S. M. Swasey, S. M. Copp, E. G. Gwinn and T. Vosch, Unusually large Stokes shift for a near-infrared emitting DNA-stabilized silver nanocluster, *Methods and Applications in Fluorescence*, 2018, **6**, 024004.
2. M. Loos, C. Gerber, F. Corona, J. Hollender and H. Singer, Accelerated Isotope Fine Structure Calculation Using Pruned Transition Trees, *Analytical Chemistry*, 2015, **87**, 5738-5744.
3. M. B. Liisberg, Z. Shakeri Kardar, S. M. Copp, C. Cerretani and T. Vosch, Single-Molecule Detection of DNA-Stabilized Silver Nanoclusters Emitting at the NIR I/II Border, *The Journal of Physical Chemistry Letters*, 2021, **12**, 1150-1154.
4. W. Kabsch, XDS, *Acta Crystallographica Section D*, 2010, **66**, 125-132.
5. D. Liebschner, P. V. Afonine, M. L. Baker, G. Bunkoczi, V. B. Chen, T. I. Croll, B. Hintze, L.-W. Hung, S. Jain, A. J. McCoy, N. W. Moriarty, R. D. Oeffner, B. K. Poon, M. G. Prisant, R. J. Read, J. S. Richardson, D. C. Richardson, M. D. Sammito, O. V. Sobolev, D. H. Stockwell, T. C. Terwilliger, A. G. Urzhumtsev, L. L. Videau, C. J. Williams and P. D. Adams, Macromolecular structure determination using X-rays, neutrons and electrons: recent developments in Phenix, *Acta Crystallographica Section D*, 2019, **75**, 861-877.
6. M. C. Burla, R. Caliandro, B. Carrozzini, G. L. Cascarano, C. Cuocci, C. Giacovazzo, M. Mallamo, A. Mazzone and G. Polidori, Crystal structure determination and refinement via SIR2014, *Journal of Applied Crystallography*, 2015, **48**, 306-309.
7. P. Emsley and K. Cowtan, Coot: model-building tools for molecular graphics, *Acta Crystallographica Section D*, 2004, **60**, 2126-2132.
8. P. Emsley, B. Lohkamp, W. G. Scott and K. Cowtan, Features and development of Coot, *Acta Crystallographica Section D*, 2010, **66**, 486-501.